

Chronic oxytocin administration in older men modulates functional connectivity during animacy perception

Pedro A. Valdes-Hernandez^{a,b,c,*}, Rebecca Polk^a, Marilyn Horta^a, Ian Frazier^a, Eliany Perez^a, Marite Ojeda^a, Eric Porges^d, Yenisel Cruz-Almeida^{b,c}, David Feifel^e, Natalie C. Ebner^{a,c,d,f,*}

^a Department of Psychology, College of Liberal Arts and Sciences, University of Florida, FL, USA

^b Department of Community Dentistry & Behavioral Sciences, College of Dentistry, University of Florida, FL, USA

^c Pain Research and Intervention Center of Excellence, University of Florida, FL, USA

^d Department of Clinical and Health Psychology, College of Public Health and Health Professions, University of Florida, FL, USA

^e Department of Psychiatry, University of California, San Diego, CA, USA

^f Department of Aging and Geriatric Research, Institute on Aging, University of Florida, FL, USA

ARTICLE INFO

Article history:

Received 18 December 2020

Revised 12 September 2021

Accepted 14 September 2021

Available online 1 October 2021

Keywords:

Intranasal oxytocin administration

Aging

Animacy perception

Heider-Simmel Task

Threshold free cluster enhancement

Ventral visual stream

Brain networks

Placebo

ABSTRACT

While aging is associated with social-cognitive change and oxytocin plays a crucial role in social cognition, oxytocin's effects on the social brain in older age remain understudied. To date, no study has examined the effects of chronic intranasal oxytocin administration on brain mechanisms underlying animacy perception in older adults. Using a placebo-controlled, randomized, double-blinded design in generally healthy older men (mean age (SD) = 69(6); $n = 17$ oxytocin; $n = 14$ placebo), this study determined the effects of a four-week intranasal oxytocin administration (24 international units/twice a day) on functional MRI (fMRI) during the Heider-Simmel task. This passive-viewing animacy perception paradigm contains video-clips of simple shapes suggesting social interactions (SOCIAL condition) or exhibiting random trajectories (RANDOM condition). While there were no oxytocin-specific effects on brain fMRI activation during the SOCIAL compared to the RANDOM condition, pre-to-post intervention change in the SOCIAL-RANDOM difference in functional connectivity (FC) was higher in the oxytocin compared to the placebo group in a network covering occipital, temporal, and parietal areas, and the superior temporal sulcus, a key structure in animacy perception. These findings suggest oxytocin modulation of circuits involved in action observation and social perception. Follow-up analyses on this network's connections suggested a pre-to-post intervention decrease in the SOCIAL-RANDOM difference in FC among the placebo group, possibly reflecting habituation to repeated exposure to social cues. Chronic oxytocin appeared to counter this process by decreasing FC during the RANDOM and increasing it during the SOCIAL condition. This study advances knowledge about oxytocin intervention mechanisms in the social brain of older adults.

© 2021 The Author(s). Published by Elsevier Inc. This is an open access article under the CC BY-NC-ND license (<http://creativecommons.org/licenses/by-nc-nd/4.0/>).

* Corresponding authors at: Community Dentistry & Behavioral Science, College of Dentistry, Pain Research and Intervention Center of Excellence, University of Florida, P.O. Box 112250, Gainesville, FL 32611, USA (A. Valdes-Hernandez). Department of Psychology, College of Liberal Arts and Sciences, Pain Research and Intervention Center of Excellence, University of Florida, P.O. Box 112250, Gainesville, FL 32611, USA (N.C. Ebner).

E-mail addresses: pvaldeshernandez@dental.ufl.edu (P.A. Valdes-Hernandez), natalie.ebner@ufl.edu (N.C. Ebner).

Introduction

The brain mechanisms underlying social cognition have been less investigated in older than younger adults, despite growing behavioral evidence of age-related change in social cognition [26,43,73,82]. This evidence cautions against direct generalization of brain research findings from younger to older individuals. Among the possible mechanisms of age-related differences in social cognition are neurochemical changes that regulate social behavior and processing, such as pertaining to oxytocin (OT) [28,46,73,75], a hypothalamic nine amino-acid peptide that modulates human cognition and behavior [37,51], including in social contexts [8,79]). Surprisingly, human research on the OT system has only recently suggested the incorporation of older individuals [46]. This novel line of investigation has already provided first supporting evidence of significant effects of intranasal OT administration on behavior related to social cognition in older adults [[17,27,26,46]; but see [34,35] for null findings].

The goal of this paper was to advance understanding of OT modulation on brain mechanisms underlying social-cognitive processes in older adults. We commenced this endeavor by selecting a crucial hallmark of social cognition: *animacy perception*, which is the tendency to confer behavior that is exclusive to living things (e.g., emotions, intentions) also to non-living or inanimate objects based on their complicated motion [41,42]. This phenomenon is basic, also manifesting in other mammals [1,5,50,72]. Animacy perception does not require active and conscious behavior to occur. Current evidence in younger adults provides supports that animacy perception is modulated by OT. For example, single-dose intranasal OT administration enhanced anthropomorphizing of moving shapes that suggest a “social story” (social condition), but not for random motion [76]. Single-dose intranasal OT administration also resulted in greater endorsement of social movement as representing “friendly social interactions” [40]. At the neurobiological level, in younger adults, OT has been observed to modulate animacy perception-related activation [40,49,58] and connectivity [32] of several brain areas, such as the inferior frontal gyri and the right superior temporal sulcus (STS). Given evidence of age-related reduction of fMRI activation in these areas [65], here we set out to test specifically whether OT affects the brain mechanisms underlying animacy perception in older adults.

To characterize brain mechanisms, we utilized functional Magnetic Resonance Imaging (fMRI), a technique that has started to unfold the neurobiology of OT action on social behavior [10,25,33,78]. Indeed, fMRI has already proven useful in revealing the modulatory effects of OT on brain mechanism related to animacy perception in younger adults. For example, levels of OT receptor gene (*OXTR*) methylation correlated with fMRI activity related to animacy perception of moving shapes—using the Heider-Simmel Task [42]—in the left STS and cingulate gyri [49]. In the same task, higher plasma OT levels were associated with enhanced fMRI activity in the left temporoparietal junction, left posterior STS (pSTS), and prefrontal

cortex [58]. Moreover, single-dose intranasal OT modulated fMRI activation related to animacy perception of moving shapes (e.g., in early visual cortex and motion processing regions such as pSTS and parietal cortex [40]). Despite this, to our knowledge, no study has used fMRI to examine OT effects on the brain during animacy perception in older adults. Also, to date, only two publications have used fMRI to examine the effects of acute intranasal OT on resting-state fMRI [25] and on fMRI during a facial emotion identification task [47] in older adults.

Intranasal OT offers a practical and effective way to investigate OT effects in the central nervous system since this administration route circumvents the blood–brain barrier and taps into central functions [13,59,62,67,68]. But to date, fMRI studies almost exclusively utilized single-dose intranasal OT administration, typically 24 or 40 international units (IUs) [36,52], despite evidence of substantially different effects on the brain and cognition between single-dose and repeated (chronic) OT administration [66,71], which supports that chronic OT administration could prove more useful in the determination of longer-term OT effects on social behavior. In particular, the examination of chronic OT effects in older adults is virtually inexistent [see Horta et al. (2020) [45] for an overview]. To our knowledge, only one study has used chronic intranasal OT administration (over 10 days in a randomized, double-blinded, placebo-controlled design with 40 IUs daily) on health-related outcomes in older adults [7] and no study has investigated such chronic OT effects on fMRI in older adults.

There are already some antecedents on younger and middle-aged, but not older, adults of the significant effects of chronic intranasal OT administration on fMRI. One study found altered resting-state fMRI functional connectivity in younger and middle-aged adults who self-administered “off-label” intranasal OT (i.e., illegally used OT to boost positive feelings, social abilities, and sexual desire), compared to matched controls [56]. This study utilized a rather uncharacterized sample of “oxytocin misusers”, and the self-administered dose, duration, and frequency were highly variable (4 to 19 weeks, three to 21 times a week, mean dose of 35.2 IU, from 14 to 70 IU). Another study adopted a randomized placebo-controlled, crossover design in younger adults with autism spectrum disorder (ASD) and found that chronic intranasal OT administration (six consecutive weeks, 24 IU twice daily) modulated resting-state fMRI functional connectivity and connectivity related to a social judgement task [86]. However, like in most single-dose studies, fMRI scans in this study were acquired 40 min after the last intranasal OT administration, when OT plasma and brain levels are still elevated [62], making it hard to distinguish acute pharmacological OT effects from more pervasive effects that persist after the acute elevation in OT levels has subsided.

Functional MRI studies adopting chronic intranasal OT administration in which the last dose is administered hours (or even days/weeks/months) before the post-intervention imaging session are necessary to elucidate the acute-independent, pervasive neurobiological effects

of OT on social cognition. Only very recently were such long-lasting effects examined in adults with ASD in two randomized, double-blinded, placebo-controlled parallel studies. These studies found effects of repeated OT administration (four weeks, 24 IUs once daily) on fMRI resting state [2]; and fMRI activation to emotion processing from point-light biological motion [9] were detected even one year after the end of the OT intervention. This incipient literature supports the feasibility of using fMRI to study the effects of chronic OT administration on the brain.

Addressing the above identified research gaps, the present study set out to determine the effects of chronic (4-week) intranasal OT administration on brain mechanisms in older men (age range: 59–85 years) using fMRI during an animacy perception task. We focused on men only in our analysis, given evidence of OT's sex-dimorphic effects on the brain [19,30,70], including in older adults [25]. We hypothesized that chronic OT modulates brain mechanisms specific to animacy perception in older adults. These brain mechanisms are characterized by fMRI activity and functional connectivity of areas that activate to animacy perception. We thus examined this OT modulation in well-circumscribed brain Regions-of-Interest (ROIs) that activate to animacy perception in older adults. This ROI restriction was informed by literature in younger adults demonstrating the ability of OT to target specific areas of the social brain [10], and in particular by OT's ability to affect both behavioral and mechanistic aspects of animacy perception as described above. Given that we examined a poorly characterized population, we determined the ROIs based on our sample's fMRI data before the intervention (at baseline), rather than based on previous reports of activations to animacy perception in younger individuals.

We examined OT modulation of animacy perception in older adults both in fMRI activation and in functional connectivity. With this approach, we extended beyond a limited localizationist fMRI activation approach, based on evidence that brain regions do not work in isolation but that networks of brain regions work in concert for complex function (van den Heuvel and Hulshoff Pol, 2010). In line with this notion, there is growing evidence of OT modulation on functional connectivity (Dodhia et al., 2014; Sripatha et al., 2013 [25,78]). In fact, OT could modulate spatiotemporal co-activation patterns between brain regions, while not modulating the amplitude of these regions' task-induced hemodynamic responses. Thus, an isolated brain region approach is not sufficient to fully capture OT mechanisms of action, and examination of fMRI activation and functional connectivity, as undertaken here, can offer different yet complementary information.

Of note, the present analysis was not designed to examine brain-behavior relationships and did not measure behavioral outcomes related to animacy perception (e.g., endorsement or evaluation of social content). Also, as a first step along this novel investigative line, our examination was focused on older adults only, to demonstrate proof-of-concept and to pave the way for future studies aiming at directly comparing younger and older individuals.

Materials and methods

Participants

This is the first neuroimaging analysis from a placebo-controlled, randomized, double-blinded, between-subject clinical trial (ClinicalTrials.gov identifier: NCT02069431; Oxytocin Aging Study), designed to investigate the effects of 4-week intranasal OT administration on physical, cognitive, and socioemotional functioning in generally healthy older adults. A CONSORT-format diagram [Fig. 1; see also Rung et al. (2021) [74]] shows the flow of participants in the larger project, including all participants who passed an initial phone pre-screening and were subsequently enrolled in the clinical trial. For the present analysis we only utilized data from older men with valid MRI data (see details below).

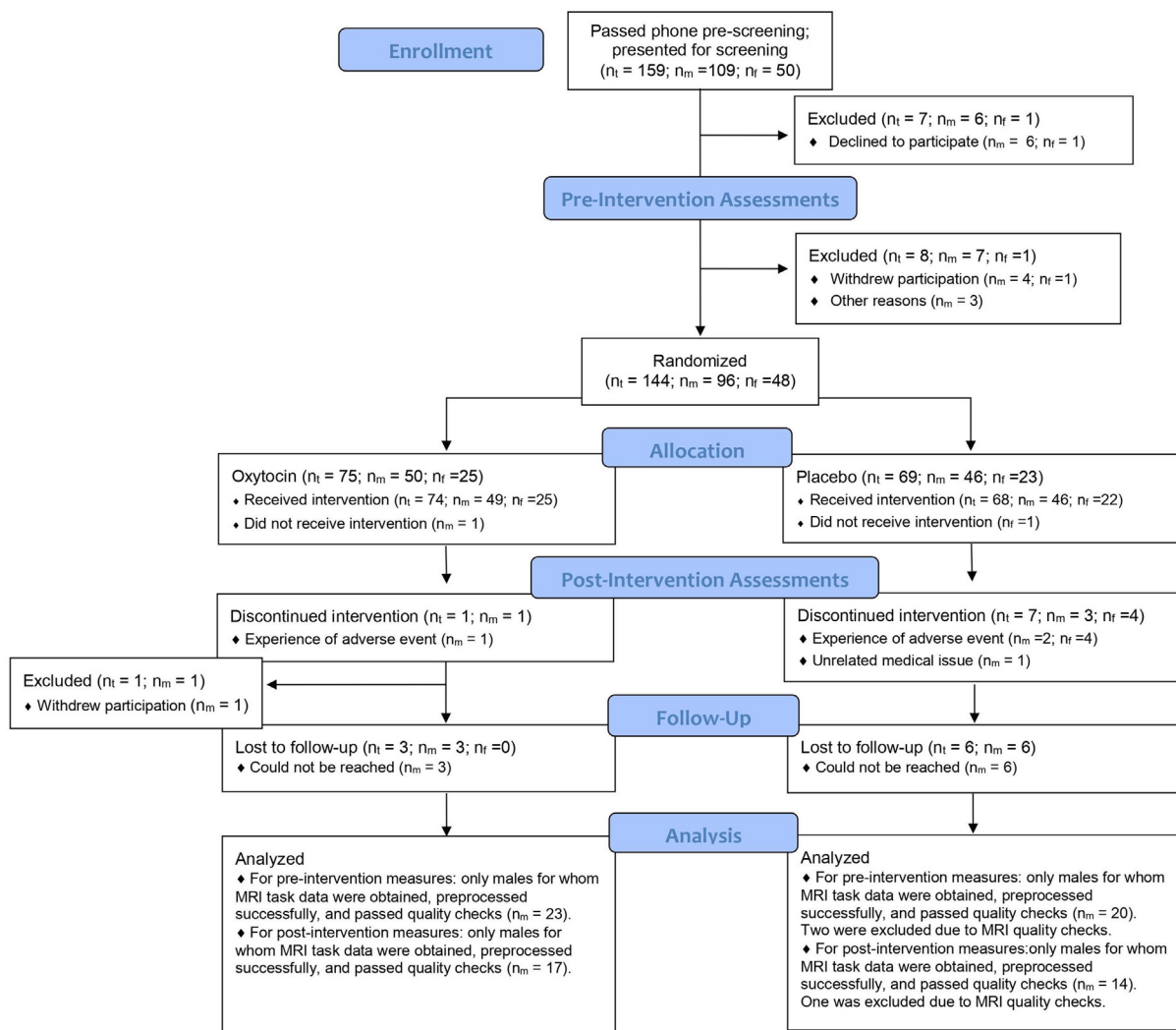
The study was conducted at the University of Florida (UF) (Department of Psychology, Institute on Aging, and McKnight Brain Institute). Participants were recruited through two UF participant registries particularly geared towards older adults and community-outreach techniques such as the Clinical and Translational Sciences Institute HealthStreet recruitment service, radio broadcasts, as well as handouts and flyers at senior citizen homes, community agencies, and churches. Participants had to be 55 years or older, English speakers, eligible to self-administer OT and for MRI as determined in a lab-internal Health Demographics Screener, score ≥ 30 on the Telephone Interview for Cognitive Status [TICS; Brandt et al. (1988) [15]], be in generally good health, without a history of primary degenerative neurological disorders, and willing and able to give informed consent. Individuals were ineligible for the study if they had a history of hyponatremia or syndrome of inappropriate antidiuretic hormone secretion; used vasoconstrictors (e.g., desmopressin, pseudoephedrine, or antidiuretic medication); had pre-treatment low sodium (<134 mEq/L) coupled with high urine osmolality (>1200 L); had psychogenic polydipsia; had a blood pressure of $>180/100$ mm; and/or engaged in heavy cigarette smoking or alcohol consumption [for details see Rung et al. (2021) [74]].

The present analysis was based on data collected from 45 men ($M = 70.9$ years, $SD = 7.1$ years, range: 59–85 years) who completed the animacy perception task at the pre-intervention MRI visit (PRE). Of those 45 participants, 34 ($n = 17$ OT; $n = 17$ placebo) also completed the animacy perception task at the post-intervention MRI visit (POST)¹. As described in more detail in the section 'Preprocessing for fMRI activation and connectivity analysis', excessive motion and global functional MRI BOLD signal change led to removal of three participants in the placebo (P) group, two at PRE and one at POST, resulting in a final sample of 31 participants ($n = 17$ OT; $n = 14$ P). Table S1 in the [Supplementary Materials](#) summarizes descriptive information regarding demographics, health, cognition, and socioemotional functioning of the sample in this analysis. As shown in

¹ Technical difficulties (e.g., with the projection system and/or the task program) prevented us from collection of animacy perception task data in all MRI-eligible participants.



CONSORT 2010 Flow Diagram



Note: Subscripts t, f, and m, refer to total sample, females, and males, respectively.

Fig. 1. CONSORT flow diagram. MRI scanning was performed at both pre-intervention (PRE) and post-intervention (POST). Forty-three participants passed MRI quality check at PRE and were used for the SPM activation analysis. Of these, 32 completed the POST MRI. One participant in POST did not pass MRI quality check and was not further considered in the analysis.

Table S1, the treatment groups (OT vs. P) did not differ in any of these variables.

Study procedures

The study protocol was approved by the UF IRB. Interested individuals underwent a phone prescreening to determine general study eligibility pertaining to targeted

age range, general health, cognitive status, as well as MRI and OT administration eligibility. Eligible participants attended a screening visit on campus starting with written informed consent and collection of information about education, household characteristics, cognitive functions, and health history. Participants also underwent a brief physical exam with the study clinician and provided urine and blood samples. Over the following 1–2 weeks, participants came to campus for four pre-intervention visits (PRE) that

comprised extensive assessment of cognitive and socio-emotional functioning (see Table S1 in the [Supplementary Materials](#) for select measures considered as sample descriptive here) as well as physical, auditory, vision, and sensory testing (not considered in this paper). The fourth pre-intervention visit comprised MRI which included fMRI image acquisition during animacy perception (see below for details regarding the Heider-Simmel Task and the MRI protocol).

A 4-week intervention phase followed in which participants self-administered, via intranasal spray, either 24 IUs of synthetic oxytocin (OT group) or a placebo (P group; containing all ingredients of the active spray except the OT), with a randomized, double-blinded assignment. The synthetic OT and P were compounded and dispensed at UF's Investigational Drug Service under IND 100,860 (sponsor: Dr. Feifel, University of California, San Diego). The 24 IUs dose was administered twice a day at home, at 7-9AM and again at 5-7PM for a total of 48 IUs/day, following standard nasal spray administration procedures [36]. Choice of this regime was based on both the rich single-dose intranasal OT administration literature and a growing literature on repeated intranasal OT administration as well as OT effects in older adults. In particular, each intake in the present study was 24 IUs, which is a common minimum dose in single-dose studies [typically between 24 and 40 IU, though it has been as low as 8 IU in humans [36,45,69]]. Multiple daily dosing is likely needed to sustain any effect of OT, as the increase in OT levels in the periphery and the brain following intranasal administration is relatively short, i.e., 104 min [62]. Our study is one of the first to administer repeated doses of OT for more than a week in healthy older adults (see also [7]). This approach is more representative of long-term treatment [61], and we recently demonstrated that it is well-tolerated in older adults [74]. It is important to note that, by the time of the submission of this publication, new evidence has shown that OT administration every other day might have stronger impact on the brain [55].

As reported in detail in Rung et al. (2021) [74], during the administration period of the study, participants received weekly follow-up calls (and one final call 7 days after the last administration) to inquire about any side effects and potential issues with the nasal spray. Participants also documented via a take-home log their nasal spray adherence for each day by noting whether they administered the nasal spray on the morning and evening of each day and the time in which the spray was administered. Additionally, at the end of the study, nasal spray bottles were returned, and spray adherence was measured by calculating an approximate proportion of the OT/P spray administered from the nasal spray bottle weights. Our data supported that the chronic OT administration was safe and well-tolerated in our sample of generally healthy older men, having no significant impact on cardiovascular, urine, or serum measures. Adverse events reported for both OT and P were few, inconsistent, and generally mild. OT did not significantly increase the likelihood of reporting adverse events, nor the number or severity of adverse events reported.

In the fourth week of the intervention phase, participants returned to campus for four post-intervention visits

(POST) that were identical to the visits prior to the intervention. For post-intervention visits, participants were instructed to not administer the spray the morning of the test sessions. This was done to allow dissociation of acute from chronic effects, since the time between the last intranasal spray administration and the test session was significantly longer than the expected time for the administered OT to be present in the blood or central nervous system [62]. Thus, any significant fMRI difference between OT and P would not be the result of acute pharmacological OT effects during the fMRI scan, but rather reflective of more pervasive effects induced by chronic OT administration. At study closure, participants were reimbursed.

Animacy perception paradigm

We used the Heider-Simmel Task [42], adapted by Castelli et al. (2000) [18] and Schultz et al. (2003) [77]. This passive viewing paradigm has been shown to recruit brain areas involved in social perception (e.g., attribution of animacy and social interactions) and theory of mind [24,38,48,58,85] such as the STS, and occipital and temporal areas. As noted above, these brain areas are targets of intranasal OT administration [33,78]. Moreover, the Heider-Simmel paradigm utilized here had previously demonstrated associations between higher endogenous (plasma) OT levels and enhanced fMRI activity in the left temporoparietal junction, left pSTS, and prefrontal cortex [49,58].

Participants passively viewed 16-sec video clips of simple moving geometric shapes (i.e., a triangle, a circle, and a diamond; all in white on black background; Fig. 2). There was a white empty square in the middle of the screen that occasionally opened to let the shapes go inside. The paradigm comprised two conditions: a SOCIAL condition, in which the moving shapes suggested goal-directed behavior/social interaction; and a RANDOM condition, in which the shapes moved without suggesting goal-directed behavior/social interaction, at an average speed comparable to that in the SOCIAL condition. The conditions were alternated and separated by an inter-trial interval (mean jittered duration of 15-17 s) during which a white fixation cross was presented in the middle of the screen (FIXATION condition). There were 8 trials for SOCIAL, 8 trials for RANDOM, and a FIXATION trial after each of them, totaling 16 FIXATION trials. The total time of the paradigm was 8 min and 44 s, after including 1 s of fixation before the first video clip and 11 s after the last video clip. Two presentation orders (reversed sequence; starting with either the SOCIAL or the RANDOM condition, respectively) were counterbalanced across participants, with identical presentation orders at PRE and POST within-subject. The paradigm was programmed in EPRIME 2.0 (Psychology Software Tools, Pittsburgh, PA).

MRI acquisition

Brain imaging took place at the McKnight Brain Institute on a 3 T Philips Achieva MR Scanner (Philips Medical Systems, Best, The Netherlands) using a 32-channel head

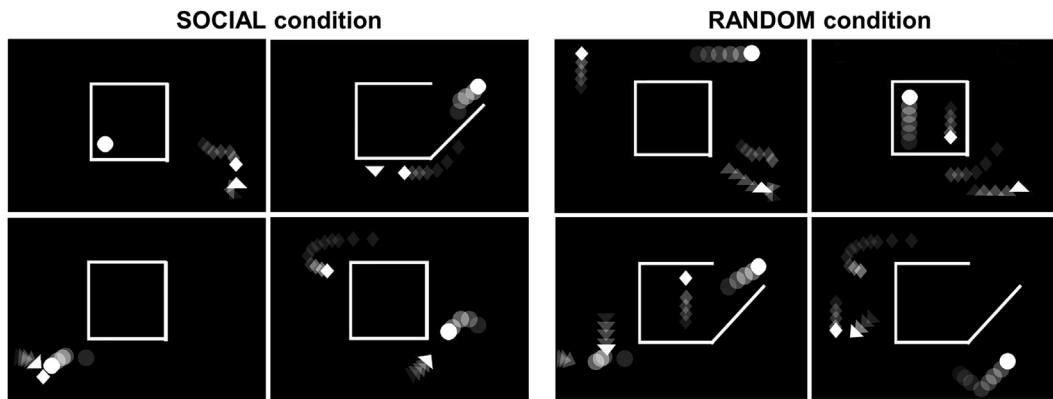


Fig. 2. Heider-Simmel Task [18,42]. The animations in the SOCIAL condition (8 trials) suggested goal-directed social interactions, e.g., confrontation, rendezvous, chasing each other, hiding, capture or release, or escaping. The animations in the RANDOM condition (8 trials) showed the shapes randomly and predictably moving, bouncing around the field of view in straight paths, like billiard balls. Average velocity and overall amount of motion was kept comparable across the SOCIAL and RANDOM conditions.

coil. During the animacy perception paradigm, gradient-echo-planar imaging (EPI) data (fMRIs) were acquired with 38 Philips-interleaved slices, TR = 2 s, TE = 30 ms, FOV = $252 \times 252 \times 133$ mm, $80 \times 80 \times 38$ matrix, flip angle of 90° , in plane resolution of 3.15×3.15 mm, slice thickness of 3.5 mm, 0 mm skip and SENSE factor of 2 in the AP direction. The run lasted 9 min and 12 s (including 4 dummy scans), and 272 time points were acquired, though only 262 time points were used for analysis (duration of the animacy perception paradigm). Whole-brain high-resolution three-dimensional T1-weighted anatomical images were also acquired using an MP-RAGE sequence with sagittal plane, FOV = $240 \times 240 \times 170$ mm, $1 \times 1 \times 1$ mm isotropic voxels, TR = 7.1 ms, TE = 3.2 ms, and flip angle = 8° .

Preprocessing for fMRI activation and functional connectivity analysis

We preprocessed the fMRI data using standard SPM12 (www.fil.ion.ucl.ac.uk/spm) pipelines for slice timing and motion/unwarp correction. We used SPM12's *unified segmentation* [4] to segment time averaged fMRIs into gray/white matter and cerebrospinal fluid and to spatially normalize them to the MNI space—a procedure known as “direct normalization”, more suitable when no field maps are available to correct for distortion related to field inhomogeneity. Given remaining age-related morphometric variability in the sample, we refined the normalization with SPM12's default DARTEL [3] to generate sample-specific template segmentations in the MNI space with a final resolution of $3 \times 3 \times 3$ mm. Since DARTEL delivers large deformations, we used the *pushforward* warping method to preserve all data from the native fMRIs. This method naturally furnished spatially (i) non-smoothed and (ii) smoothed fMRIs with a 6-mm kernel, which were used as inputs in the fMRI activation and functional connectivity analyses described below. We applied the same DARTEL procedure independently to the T1-weighted images. Gray matter, white matter, and cerebrospinal fluid masks were

eroded with a binarization threshold of 0.3, 0.5, and 0.5, respectively, one erosion step and one erosion neighbor.

Using CONN version 19a [87], we calculated temporal *noise regressors* for denoising the data. These comprised six motion parameters and their temporal derivatives, the *scrubbing* penalizing artifactual time points (acquisitions with frame-wise displacement above 0.9 mm or global BOLD signal changes above 5 standard deviations were flagged as potential outliers), and the first five spatial principal components of the spatially non-smoothed preprocessed fMRIs within white matter and cerebrospinal fluid (*aCompCor*). We also calculated six temporal *condition regressors*: boxcar functions corresponding to the SOCIAL and RANDOM conditions, convolved with the canonical hemodynamic response function (HRF), and the first and second temporal derivatives of the HRF, to account for departures from canonical behavior.

Functional MRI quality control (QC)

We examined the quality of the fMRIs using CONN version 19a. We band-pass temporal filtered the fMRIs between 0.008 and 0.09 Hz and regressed out noise and condition regressors using the general linear model (GLM). Visually based QC was based on comparison, before and after denoising, of the histograms of temporal correlation between random 1,000 brain voxels of the preprocessed fMRIs; and inspection of the carpet plots of the BOLD signal in all voxels. Using permutations, we evaluated departures from the null distribution of the correlation between the functional connectivity in random 1,000-node networks and brain displacements; and between the former and the global signal change [22].

Further, we calculated the change in global signal (GS) time-series and the frame-wise displacement (FD) time-series, from the realignment parameters, as implemented in the CONN 19a toolbox (based on the ART toolbox; https://www.nitrc.org/projects/artifact_detect/). In particular, we calculated four second-level QC variables: mean and maximum QC-GS and mean and maximum QC-FD. We then inspected, after time-point outlier removal, the

violin plots of mean QC-GS and mean QC-FD to detect participants with data outside three times the interquartile range of their sample distribution. As noted above, this QC procedure led to the removal of three participants in the P group, two at PRE and one at POST. Finally, we performed a *t*-test of the PRE-to-POST difference of mean and maximum QC-GS and mean and maximum QC-FD to test if there were significant changes in artifacts and motion that could drive or confound the analysis. All tests were not significant ($p = 0.64$, $p = 0.19$, $p = 0.25$, and $p = 0.33$ for mean QC-GS, maximum QC-GS, mean QC-FD, and maximum QC-FD, respectively).

Statistical parametric map (SPM) of fMRI activation (and deactivation)

The first step to test our hypothesis was to determine the voxels (SPM) that activated to animacy perception. This was done by fitting whole-brain gray matter voxel-wise univariate GLM to the spatially smoothed preprocessed fMRIs, obtained as described above, for the 43 participants who survived image QC at PRE, after high-pass temporal filtering from 0.0078 Hz. All above-defined noise and condition regressors were included in the first level GLM design matrix, the former as nuisance covariates and the latter as predictors of interest. Following the summary statistics approach to the second-level analysis [31], we computed an SPM of the one-sample *t*-test of significance of the average of the 43 individual SOCIAL-RANDOM contrasts, with significance set at $p < 0.0005$ (two-tailed), corrected for multiple comparisons at the voxel level using

False Discovery Rate (FDR). This yielded voxels that activated and deactivated to animacy perception (i.e., positive and negative SOCIAL-RANDOM). An extra layer of type I error control was added by scrubbing relatively scattered clusters of voxels of the same SOCIAL-RANDOM sign no bigger than 20 voxels. The SPM resulting from this analysis can be found in [Figure S1](#) of the [Supplementary Materials](#).

Definition of regions of interest (ROI) for ROI-to-ROI fMRI functional connectivity

Our analysis was guided by our hypothesis that OT modulates brain mechanisms in areas known to activate to the SOCIAL compared to the RANDOM condition. Thus, each pair of connected ROIs in the fMRI functional connectivity analysis included at least one ROI exclusively formed by brain voxels where the above-described group-level SPM (significant averages of the 43 individual SOCIAL-RANDOM contrasts at PRE) was significantly positive (i.e., the positive SPM). We called these the 'positive ROIs'. The extent of continuous brain areas with positive SPM were large enough (see [Figure S1](#) in the [Supplementary Materials](#)) to render unsupervised clustering methods invalid for defining the positive ROIs. Under the unsupervised clustering methods, the positive ROIs resulted in excessively large regions comprising several anatomical areas known to be related to different brain mechanisms. Thus, we parcellated the positive SPM into ROIs using the anatomical BRAINNETOME atlas [29], a structural connectivity-based parcellation of the human brain with 246 cortical and subcortical structures ([Fig. 3A](#)). Of note,

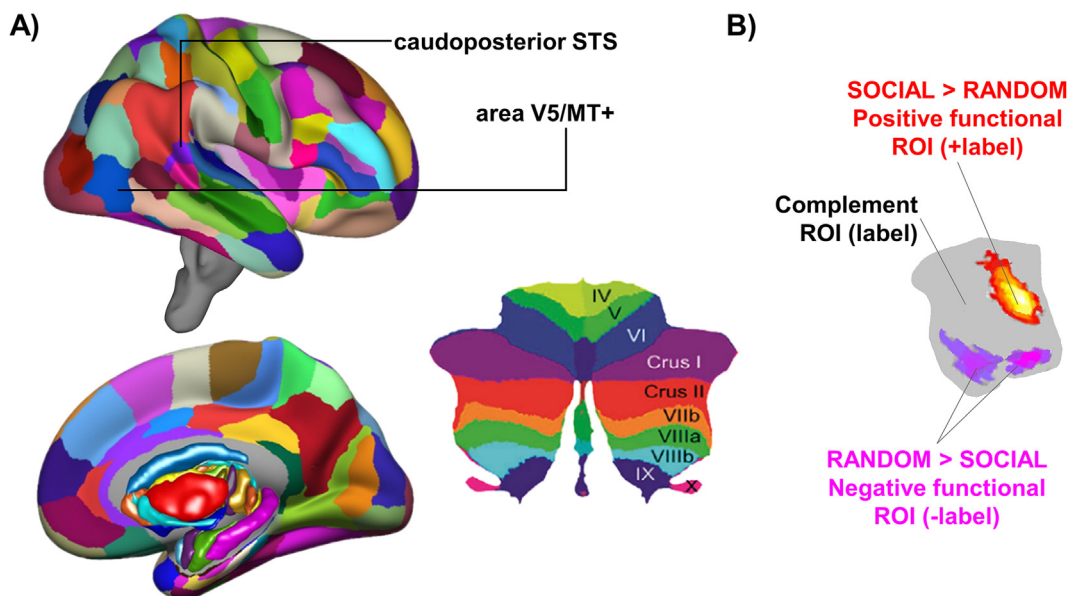


Fig. 3. ROIs used for functional connectivity analysis. Panel A) Structural regions of interest (ROIs) were defined with the anatomical BRAINNETOME atlas [29], with 246 cortical and subcortical structures; complemented with the 26 cerebellar structures of the AAL atlas [84] and the brainstem of the FSL Harvard-Oxford atlas cerebellar areas. Panel B) SPM12 summary statistics analysis on individual SOCIAL-RANDOM contrasts of 43 participants who survived image quality control at PRE (pre-intervention) showed that a subset of structural ROIs contained non-overlapping areas of activation and/or deactivation (i.e., significant main effect of condition at PRE); these non-overlapping areas were used to create positive and negative functional ROIs, respectively. Positive (negative) ROIs were labeled "+label" ("-label"), where "label" references the parent ROI. The remaining non-activated ROI of the larger structural ROI, if bigger than 20% of the size of the parent ROI, was termed complement ROI and labeled after the parent ROI. STS = superior temporal sulcus. V5/MT+=V5 or middle temporal complex (motion area).

the BRAINNETOME atlas maps structures to behavioral domains and experimental paradigms, following the Brain-Map taxonomy [57], facilitating functional interpretation of results. It involves regions crucial in animacy perception, such as the (caudal and rostral) pSTS [48,20,85] and the visual area V5/MT+ [24,44]. It does not, however, contain the brainstem and the cerebellum. That is why we augmented the BRAINNETOME by adding the brainstem of the FSL Harvard-Oxford atlas² and the 26 cerebellar structures of the AAL atlas [84]³.

To account for all possible connections to these positive ROIs, we expanded the whole space of analysis by incorporating 'negative ROIs', i.e., BRAINNETOME-based parcellations of the negative SPM. We labeled the positive and negative ROIs as 'functional ROIs'. Positive and negative ROIs within the same BRAINNETOME structural area may have distinct functional roles. Thus, to increase the sensitivity of our analysis, they were treated as functionally independent ROIs. The remaining region within each structural ROI, that was neither positive nor negative, was labeled the 'complement ROI'. Structural ROIs and complement ROIs coincided when the former contained no functional ROIs. Fig. 3B illustrates these subdivisions within a BRAINNETOME structure. Table S2 in the [Supplementary Materials](#) shows all ROIs (i.e., positive, negative, and complement) and their volumes.

Functional MRI connectivity was calculated from each positive functional ROI to all functional and complement ROIs. Thus, we excluded all connections that did not include at least one positive ROI. Given $N_p = 35$, $N_n = 34$, and $N_c = 265$ for the number of positive, negative, and complement ROIs, respectively, our space of analysis was the Cartesian product of N_p ROIs with $N_p + N_n + N_c$ ROIs. Auto-connections were also excluded, including connections from functional ROIs to their own complement ROIs, due to their proximity.

Estimation of ROI-to-ROI fMRI functional connectivity

We used CONN version 19c to calculate the spatial average of the spatially non-smoothed fMRIs within the ROIs for each participant and visit (PRE, POST), excluding voxels outside the individual's gray matter mask. As with the fMRIs, we band-pass temporal filtered the resulting ROI time series between 0.008 and 0.09 Hz and regressed out noise and condition regressors using the GLM⁴. We con-

verted these denoised ROI time series to percent signal change and centered them to a mean of zero. We calculated all zero-lagged bivariate weighted correlations between the positive functional ROIs and the rest of the ROIs, for all participants, visits (PRE and POST), and conditions (SOCIAL and RANDOM). For each condition, weights were defined by the corresponding temporal condition regressor to account for contaminations across conditions associated with hemodynamic delays. Finally, we transformed these correlations to normally distributed functional connectivity measures using the Fisher transform to meet the assumptions of standard second-level GLMs. These ROI-to-ROI functional connectivity measures were used for the group-level analysis, as described next.

Group-level analysis: Chronic OT effects

Our design comprised one between-subject factor: *treatment* (OT, P) and two within-subject factors: *condition* (SOCIAL, RANDOM) and *time* (PRE, POST). In parallel models, our dependent variable was either the fMRI activation or the ROI-to-ROI functional connectivity. We tested the *treatment* \times *condition* \times *time* interaction to quantify the effect of chronic OT on functional networks specific to animacy perception. Follow-up analysis was conducted to allow for interpretation of the *treatment* \times *condition* \times *time* interaction. To that end, we tested other effects on the dependent variable for which the *treatment* \times *condition* \times *time* interaction was significant. Among the eight contrasts that this factorial design entailed (including the three-way interaction), we were interested in those reflecting changes across visits, specifically the main effect of *time*, the simple effect of the *condition* \times *time* interaction at the level *treatment* = P, and the simple effect of the *condition* \times *time* interaction at the level *treatment* = OT. By transforming the outcome at the first level to be the difference across visits (POST-PRE), we effectively retained only the partitioned errors related to time effects. This is equivalent to obtain a 2x2 design with the factors *treatment* and *condition*. In this model, the contrast of interest was the *treatment* \times *condition* interaction, and the simple effects of *condition* at *treatment* = P and *treatment* = OT were used for interpretation.

For the fMRI activation analysis, we used the recommended way to test the *treatment* \times *condition* \times *time* interaction in SPM, that is retaining only the partitioned errors related to the effects of the interaction of the within-subject factors, i.e., *condition* \times *time*. This was done by calculating the contrast (SOCIAL_{POST}-RANDOM_{POST})-(SOCIAL_{PRE}-RANDOM_{PRE}) at the subject level. The *treatment* \times *condition* \times *time* interaction was thus tested by testing the main effect of the between-subject factor *treatment* using this contrast as the dependent variable (which was equivalent to two independent samples *t*-test). We calculated this contrast at the voxel and ROI level.

Statistical significance of the group-level analysis

The statistical significance level of the effects in individual voxels or ROIs for the fMRI activation analysis and for

² http://ftp.nmr.mgh.harvard.edu/pub/dist/freesurfer/tutorial_packages/centos6/fsl_507/doc/wiki/Atlases.html

³ The full list of labels and coordinates of the BRAINNETOME ROIs can be downloaded at <https://atlas.brainnetome.org/download.html>; the full list of labels of cerebellar AAL ROIs can be downloaded at <http://www.gin.cnrs.fr/en/tools/aal/>.

⁴ Conditions regressors were regressed out to remove constant task-induced responses in the BOLD signal (default setting in CONN). Otherwise, the functional connectivity, based on the correlation between the BOLD signal of two ROIs, could be either underestimated (if the task-induced BOLD responses are present in only one of the ROIs) or overestimated (if the task-induced BOLD responses are present in both ROIs). Given the duration of the condition blocks in our experiment, the approach used in this paper is mathematically equivalent to testing generalized psychophysiological interactions (gPPI) [63]. Removing the task-induced BOLD responses is equivalent to accounting for the main psychological effect in gPPI.

the individual ROI-to-ROI connections in the fMRI functional connectivity analysis was corrected for multiple tests using FDR ($p < 0.05$, two-sides). Furthermore, as the number of simultaneous tests was large, we also applied the Threshold Free Cluster Enhancement (TFCE) statistics [80] on the ROI-to-ROI connectivity matrix, as implemented in CONN version 19c, using default parameters (i.e., $H = 2$ and $E = 0.5$). Briefly, for the fMRI functional connectivity analysis, TFCE was applied to the entire ROI-to-ROI matrix of T-statistics, with ROIs sorted using an optimal leaf ordering for hierarchical clustering based on ROI-to-ROI functional similarity [6]. The expected distribution of TFCE values under the null hypothesis was numerically estimated using 10,000 randomization/permutation iterations of the original data and used to compute for each cluster in the original analysis a peak-level Family-Wise-Error (FWE) corrected p-value (i.e., the likelihood under the null hypothesis of observing at least one or more connections with this or larger TFCE scores over the entire ROI-to-ROI connectivity matrix). Also, each local-extremum/peak in the TFCE map was compared to the null hypothesis distribution of local-peak TFCE values to calculate peak-level FDR corrected p-values [i.e., the expected proportion of false discoveries among peaks having this or larger TFCE scores across the entire ROI-to-ROI matrix; see Chumbley et al. (2010) [21]].

Results

Functional MRI activation analysis

We found no significant effects of *treatment* on the $(\text{SOCIAL}_{\text{POST}} - \text{RANDOM}_{\text{POST}}) - (\text{SOCIAL}_{\text{PRE}} - \text{RANDOM}_{\text{PRE}})$ contrast of the fMRI activation at the voxel ($p > 0.05$ FDR corrected or TFCE corrected) or ROI ($p > 0.05$ FDR corrected) level. These negative results were found irrespective of the restriction applied, i.e., after small volume correction (or masking) using the significant positive SPM (which tests our specific hypothesis), or the entire gray matter mask.

Functional MRI connectivity analysis

Fig. 4A shows the network that survived the Threshold Free Cluster Enhancement (TFCE) statistics when testing the *treatment* \times *condition* \times *time* interaction ($p < 0.05$ after FWE correction and $p < 0.01$ after FDR correction; two-tailed). Three of the connections in this network were also individually statistically significant, i.e., they survived FDR correction ($p < 0.05$; two-tailed). These were the connections (i) between the positive functional ROI within the right caudoposterior STS (right + cpSTS) and the positive functional ROI within the left extreme lateroventral Brodmann area 37 (left + A37elv); (ii) between the positive functional ROI within the right rostroventral Brodmann area 39 (right + A39rv) and the complement ROI in the right caudal lingual gyrus (right cLinG); and (iii) between the positive functional ROI within the left medial occipital gyrus (left + mOccG) and the complement ROI in the left dorsolateral Brodmann area 37 (left + A37dl). Fig. 4B shows the cortical locations of the nodes of the observed TFCE network.

The effect sizes of the *treatment* \times *condition* \times *time* interaction in the network identified using TFCE are shown in Fig. 5A (first plot). All effects were positive. This means that the functional connectivity during SOCIAL compared to RANDOM had a PRE-to-POST increase in the OT group, compared to the P group. As this can happen under different combinations of values of functional connectivity during SOCIAL and RANDOM at PRE and POST, we facilitated interpretation of this three-way interaction by estimating, using a partitioned errors model, the main effect of *time* (Fig. 5A, second plot) and the simple effects of the *condition* \times *time* interaction at the two *treatment* levels (P and OT, Fig. 5A, third and fourth plots, respectively). Using these effects, i.e., the main effect of *time* and the simple effects of the *condition* \times *time* interaction, we estimated the (fitted) simple effects of *time* for the $2 \times 2 = 4$ combinations of *condition* (two levels: RANDOM and SOCIAL) and *treatment* (two levels: P and OT; see the four plots under Fig. 5B). For example, the “fitted” simple effect of *time* at *condition* = SOCIAL and *treatment* = OT (Fig. 5B fourth plot) is equal to the main effect of *time* plus $\frac{1}{2}$ times the simple effect of the *condition* \times *time* interaction at *treatment* = OT.

The results in Fig. 5 indicate that the change in functional connectivity from PRE to POST within the observed TFCE network was higher in RANDOM than in SOCIAL in the P group, i.e., all connections have a significant negative simple effect of the *condition* \times *time* interaction in the P group (FDR corrected across the connections of the network, Fig. 5A, third plot). This effect seems to be driven by an increase in functional connectivity from PRE to POST in all connections during RANDOM (Fig. 5B, first plot) compared to only few connections during SOCIAL (Fig. 5B, second plot) for the P group. For the OT group, in contrast, the change in functional connectivity from PRE to POST was only significantly different between the *condition* levels in a small number of connections (Fig. 5A, fourth plot). This aligns with no significant change in functional connectivity from PRE to POST in the RANDOM condition (Fig. 5B, third plot) or the SOCIAL (Fig. 5B, fourth plot) condition for the OT group. This differential pattern for the P vs. the OT group is reflected in the significant *treatment* \times *condition* \times *time* interaction, that may represent a pharmacological (counteracting) effect of chronic OT administration. Fig. 5C offers a summarizing visual representation of the above-mentioned main and simple effects related to changes in functional connectivity from PRE to POST, to further aid interpretation of the *treatment* \times *condition* \times *time* interaction. In this graph, colored dots represent fitted single effects of time (blue for P, red for OT) and gray dots represent main effects of time. Slopes of lines represent the simple effects of the *condition* \times *time* interaction (blue for P, red for OT). The effects of the *treatment* \times *condition* \times *time* interaction are illustrated by the change in sign of these slopes.

Discussion

This placebo-controlled, randomized, double-blinded, between-subject study provides novel evidence that four

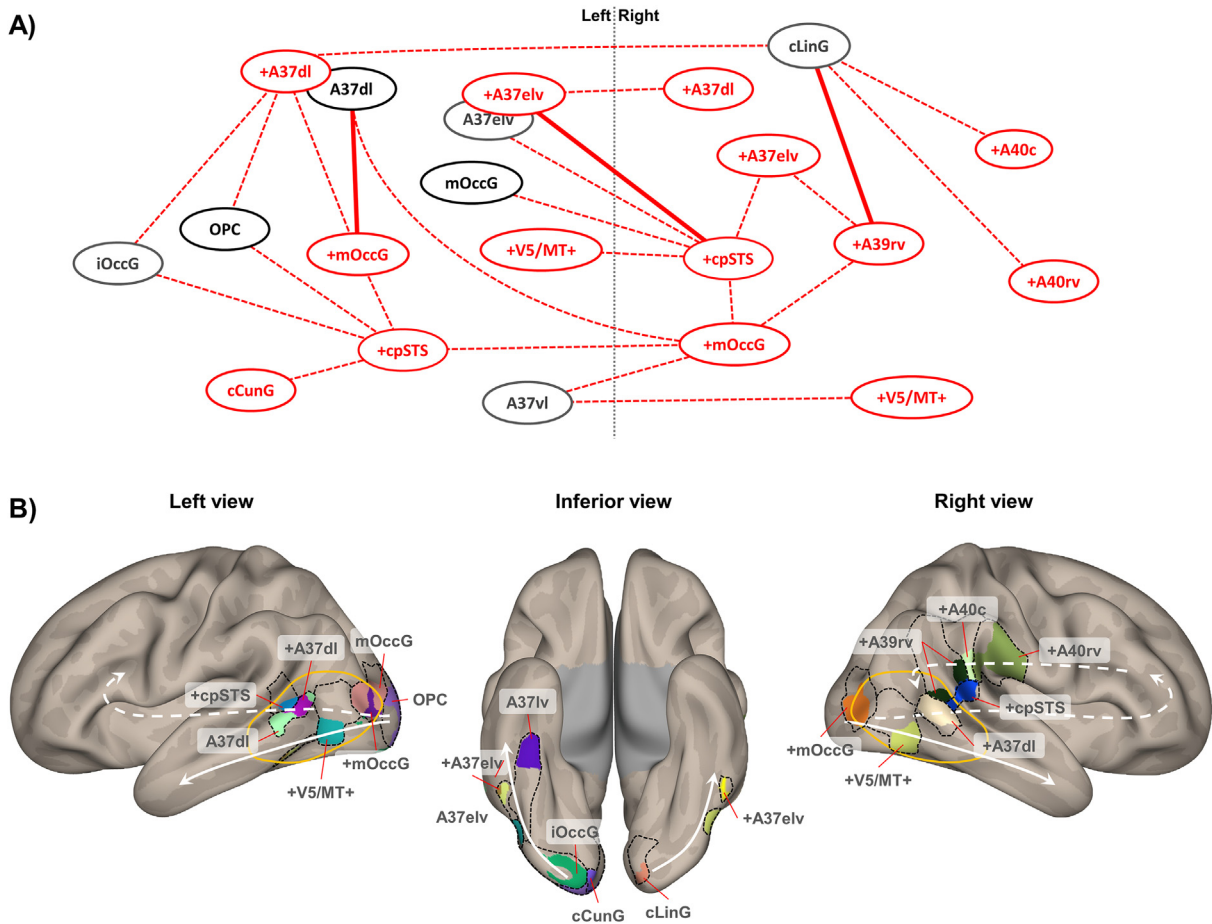


Fig. 4. Panel A) Network that survived the Threshold Free Cluster Enhancement (TFCE) statistics ($p < 0.05$ FWE corrected; two-tailed) when testing the *treatment* \times *condition* \times *time* interaction. In the graph, red links represent positive values of the *treatment* \times *condition* \times *time* interaction. Solid links represent connections that were individually significant, i.e., survived FDR correction ($p < 0.05$; two-tailed). Red and gray nodes (full circles) represent positive functional and complement ROIs, respectively. Functional and complement ROIs derived from the same anatomical structure are partially superimposed. Panel B) Anatomical location of the areas of the network. The yellow contour approximately delineates the lateral occipitotemporal cortex (LOTc). The ventral stream of visual processing is represented with solid white arrows. A bottom-up ventral subdivision of the ventro-dorsal pathway of the action observation network is represented with dashed white arrows in the left hemisphere. Bottom-up and top-down subdivisions of the same ventro-dorsal pathway of the action observation network are also represented with dashed white arrows in the right hemisphere. FWE = Family Wise Error. FDR = False-Discovery-Rate. R = right. L = left. cpSTS = caudoposterior superior temporal sulcus. A37elv, A37lv, and A37dl = extreme lateroventral, lateroventral, and dorsolateral Brodmann area 37. mOccG = medial occipital gyrus. OPC = occipital polar cortex. V5/MT+=V5 or middle temporal complex (motion area). iOccG = inferior occipital gyrus. cCunG = caudal cuneus gyrus. cLinG = caudal lingual gyrus. A39rv = rostroventral Brodmann area 39. A40c and A40rv = caudal and rostroventral Brodmann 40. (For interpretation of the references to color in this figure legend, the reader is referred to the web version of this article.)

weeks of intranasal OT versus P administration modulates MRI functional connectivity, but not fMRI activation, measured the day after the last self-administered dose, in older men during animacy perception. The OT-modulated functional network comprised areas in the bilateral occipital lobes, bilateral temporal lobes, right inferior parietal lobule, and bilateral pSTS. In particular, functional connectivity increased during the RANDOM condition and partially decreased during the SOCIAL from PRE-to-POST intervention in the absence of chronic OT administration (i.e., in the P group); while chronic OT administration appeared to counteract these effects, effectively maintaining functional connectivity values from pre- to post-intervention, and even reverting the SOCIAL versus RANDOM difference from negative to positive in some connections.

This pattern of findings supports that chronic OT acts on the connectivity of circuits involved in action observation and social perception in older men. The BrainMap taxonomy provided by the BRAINNETOME atlas maps the areas of the here identified OT-modulated network to visual attention, action observation, and social cognition [57]. Bilateral areas of the observed OT-modulated network lie in visual ventral pathways (see Fig. 4B) that promote object identification and recognition by transforming visual inputs into short-term perceptual representations of object characteristics [64], such as agency and animacy [14,54]. More dorsally, the observed OT-modulated network overlaps with the lateral occipitotemporal cortex (LOTc; see Fig. 4B), a sensory hub of action observation, specifically in areas of visual, multimodal,

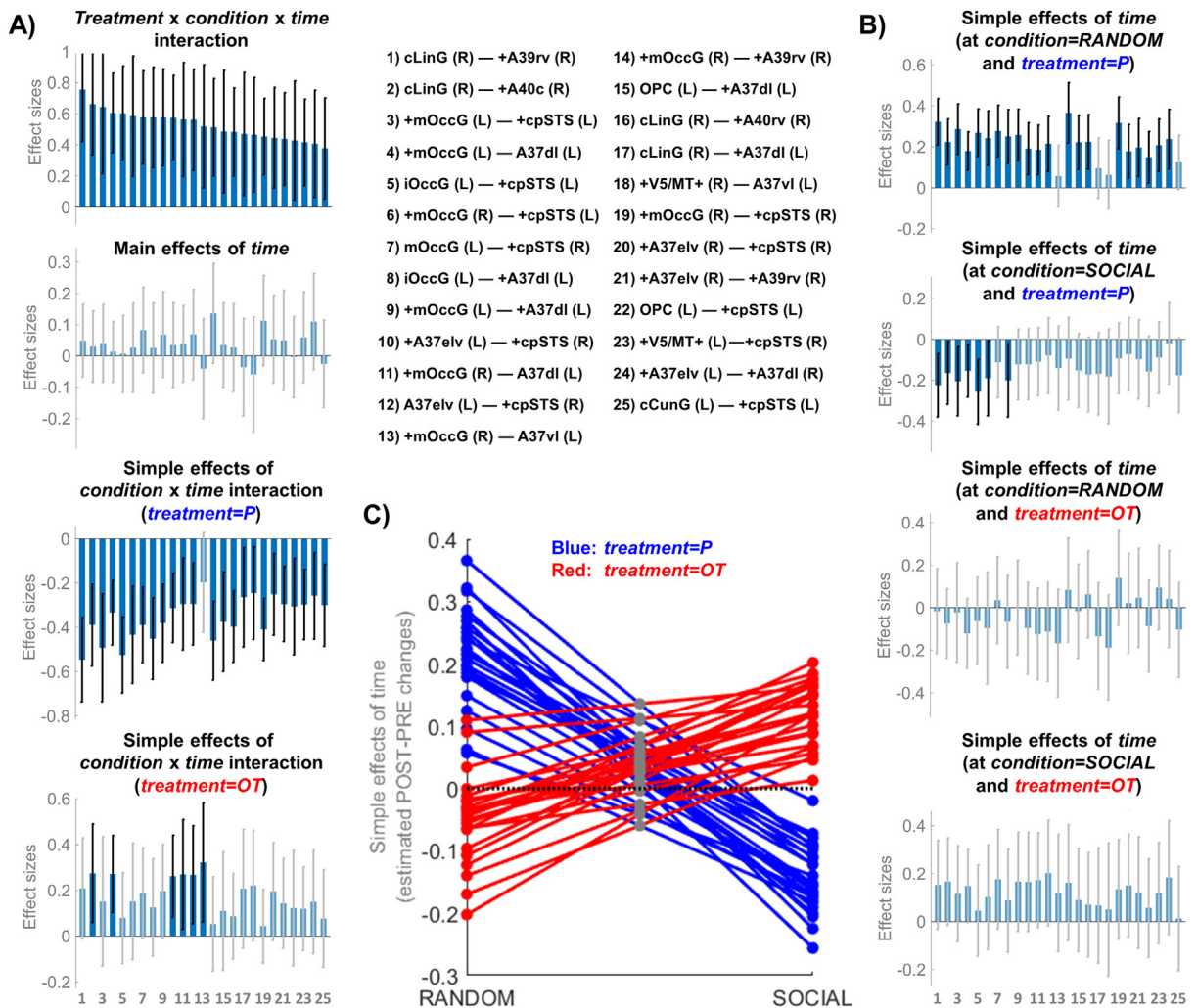


Fig. 5. Follow-up analysis and summarizing visualization of connections forming the TFCE network that survived testing the *treatment* × *condition* × *time* interaction. Panel A) Effects sizes and FDR corrected confidence intervals (CIs) of the *treatment* × *condition* × *time* interaction (first plot), the main effect of *time* (second plot), and the simple effects of the *condition* × *time* interaction at each *treatment* level (P third plot; OT fourth plot). Effects and CI bars corresponding to CIs crossing zero (indicating non-significant effects) are represented with lighter colors. Connections are sorted in descending order from the lowest (leftmost) to the highest (rightmost) effect size of the *treatment* × *condition* × *time* interaction and are numbered (see bottom plot) with their labels displayed in the middle top of the figure. Panel B) Effect sizes of fitted simple effects of *time* at each of the *condition* (RANDOM and SOCIAL) and *treatment* (P and OT) levels. Panel C) Plot summarizing the above-mentioned main and simple effects. Ordinate values are equal to effects of *time*. Blue and red dots represent fitted simple effects of *time* in all connections of the observed TFCE network at each *condition* level (RANDOM, SOCIAL) and at each *treatment* level (blue for P, red for OT). For each connection of the TFCE network, dots within a given *treatment* level (i.e., same color dots at both *condition* levels) are connected with same color lines of slopes that are equal to the simple effects of the *condition* × *time* interaction at that *treatment* level. The ordinate values of the gray dots are equal to the main effects of *time*. The abscissa value of these gray dots is halfway from RANDOM to SOCIAL to indicate they are main effects (i.e., they are the average effect of *time* across *condition* levels) and, by definition, they coincide in the intersection between the blue and red lines (i.e., they are also the average effect of *time* across *treatment* levels). TFCE = Threshold Free Cluster Enhancement. FDR = False-Discovery-Rate. R = right. L = left. cpSTS = caudoposterior superior temporal sulcus. A37elv, A37lv, and A37dl = extreme lateroventral, lateroventral, and dorsolateral Brodmann area 37. mOccG = medial occipital gyrus. OPC = occipital polar cortex. V5/MT+=V5 or middle temporal complex (motion area). iOccG = inferior occipital gyrus. cCunG = caudal cuneus gyrus. cLinG = caudal lingual gyrus. A39rv = rostroventral Brodmann area 39. A40c and A40rv = caudal and rostroventral Brodmann 40. (For interpretation of the references to color in this figure legend, the reader is referred to the web version of this article.)

and abstract representations of perceived objects and their motion [60]. Among these abstract LOTC representations, intentionality is functionally located more dorsally in our detected OT-modulated network, in the caudoposterior pSTS (cpSTS) [60]. The involvement of other bilateral areas around the pSTS suggests bottom-up and top-down modulation of the ventro-dorsal stream of an action observation network [11] (see Fig. 4B) that is likely

responsible for predictive coding of intentions and goals of actions [53].

Of particular interest is that chronic OT modulated the functional connectivity of a network containing the bilateral cpSTS and its surroundings [i.e., dorsolateral portion of bilateral Brodmann (A) area 37 (A37dl), rostrocaudal portion of right A39 (A39rc), and caudal and rostroventral portions of right A40 (A40c and A40rv); with connections

to the positive cpSTS and rostroventral portions of rostroventral A39 (A39rv) in the right hemisphere being individually significant]. This finding confirms that chronic OT acts on brain processes specifically underlying animacy perception [23,85] and the perception of social interactions, known to recruit the area where the positive A39rv and A40c are located [48]. In fact, a meta-analysis [88] and functional connectivity findings [24] support an integrative neural model that places the right cpSTS at the intersection of implicit (action observation, social perception) and explicit (theory of mind) systems of social information processing [81,88]. Our results suggest that chronic OT may have primarily affected the functional connectivity of a network that underlies the implicit system, probably affecting the role of the cpSTS in selectively extracting and decoding social content from incoming visual information to relay it to higher-level social-cognitive areas [88].

Even though our results suggest that chronic OT modulated the connectivity of areas known to be involved in animacy perception, it is not possible, and it is beyond the scope of this paper, to ascertain the impact on social behavior, since participants in the present study were not asked to provide evaluation or endorsement of the social content of the videos. Rather, this study examined basic mechanisms associated with passive viewing of animacy. However, previous work suggests that an increase in activity in areas like the pSTS and its surroundings is commensurate with the degree of social perception and other mentalizing abilities [12,18,83].

Our study importantly adds to a currently very limited literature linking fMRI brain functional connectivity to animacy perception. Only two previous fMRI-based connectivity studies have examined animacy perception [24,44]. Both studies were based on measures of effective connectivity—an advantage offered by more hypothesis-driven approaches that allow restriction to a smaller number of ROIs. In line with our findings here in older men, both studies portrayed the right pSTS as a central hub; and its ipsilateral effective connectivity (based on partial correlation) was positively correlated with animacy perception, compared to random motion [24].

Our follow-up analysis of the specific connections within the OT-modulated network showed increased functional connectivity during the RANDOM condition and reduced functional connectivity during the SOCIAL condition after P administration. This pattern of results could represent habituation or desensitization to social information in older men who did not undergo the OT intervention; possibly due to increased processing of inanimate features of the moving objects. Following the same line of reasoning, our results suggest that chronic OT intervention may counter habituation/desensitization to repeatedly presented social stimuli, boosting animacy perception. Noteworthy, habituation effects resulting from chronic OT administration have been reported in recent publications on younger participants with ASD. In particular, in the P group, fMRI activation of the bilateral pSTS during the recognition of negative emotional states from whole body point light displays, measured a day after a four-week OT (24 IU/day) administration, significantly decreased compared to baseline. In the OT group, in con-

trast, there was no such significant change or change was of smaller magnitude across brain structures [9]. Using the same sample, Alaerts et al. (2020) [2] also showed that, in the P group, resting-state fMRI functional connectivity of the amygdalae with the posterior superior and medial temporal gyri (pSTG and pMTG), also measured a day after the same administration regime, significantly changed compared to baseline, while it did not significantly change in the OT group.

Intriguingly, while chronic OT did not significantly modulate fMRI activation during animacy perception in our older men, it modulated fMRI functional connectivity. This suggests that chronic OT might not have changed the determinants of the amplitude of task-induced hemodynamic responses associated with animacy perception (e.g., energy consumption, neuro-vasculature, neurovascular couplings and neurometabolic factors), but did change the spatiotemporal pattern of co-activation between brain regions, probably reflecting neuroplastic modifications via prolonged OT administration [39].

Limitations and future research

One limitation of the present study, which calls for future independent replication, is the relatively small sample size ($n = 31$), reducing the chance of detecting small effect sizes. Also, with smaller sample sizes, the likelihood that statistically significant results reflect true effects is reduced [16]. Since this likelihood is inversely proportional to the type I error, one can protect the analysis against possible spurious positive results associated with a smaller sample size by using a stringent statistical threshold, e.g., $p < 0.01$, corrected, which is five-fold lower than typically used in exploratory analyses, that is $p < 0.05$, corrected. When doing so, our results can be considered as marginally significant when controlling at FWE ($p < 0.05$); but still remain significant when controlling at FDR ($p < 0.01$). Additionally, partitioning the variance of the errors by calculating the PRE-to-POST difference reduced subject-related variability, further increasing statistical power. Nevertheless, moving forward, a replication of the present findings in a larger sample is warranted.

Also, a direct comparison with a younger population can provide valuable information about the specificity of results in an older adult sample, and the lack of a younger adult comparison group is a limitation of the current study. Moving forward, a direct age-group comparison constitutes a fruitful next step of this line of work. For these future samples it would also be beneficial to include individuals from both sexes, utilizing measures of effective connectivity, an animacy perception paradigm that requires more engaged and cognitively effortful processing (e.g., endorsing social content in the figures) to further elucidate the mechanisms underlying chronic OT modulation in the social brain among older adults. Further, test of novel and possibly more efficient intranasal OT administration regimes is warranted. For example, recent findings by Kou et al. (2020) [55] suggest that a repeated administration every other day might have stronger effects on the brain than daily administration.

Another limitation of our study is that brain data was only assessed at baseline (PRE) and after the intervention (POST). The effects of OT on the brain could significantly vary across different time points of the intervention, e.g. just after the first intake, just after the end of the intervention or a year later [2]. It is imperative to design future studies aiming at retaining participants long enough to be able to assess long-lasting chronic OT administration effects on the brain. Finally, future work will be necessary to determine generalizability of the observed effects among clinical populations in aging (e.g., dementia, depression, social anxiety).

Conclusion

The present study is the first to examine pervasive effects of chronic OT on functional brain connectivity during animacy perception in generally healthy older men using a unique and rigorous placebo-controlled, randomized, double-blinded, between-subject study design. Advancing understanding of the role of OT in the older social brain, the present study provides intriguing novel evidence of increased functional connectivity during non-social and decreased functional connectivity during social processing among older men not treated with intranasal chronic OT; while chronic OT administration counteracted these effects, even mildly reverting the SOCIAL versus RANDOM difference from negative to positive in some connections. This pattern of findings supports the impact chronic OT has on the functional connectivity of neurocircuits involved in animacy perception in older adults.

CRedit authorship contribution statement

Pedro A. Valdes-Hernandez: Conceptualization, Methodology, Software, Formal analysis, Data curation, Writing - original draft, Writing - review & editing, Visualization. **Rebecca Polk:** Methodology, Investigation, Formal analysis, Data curation, Writing - original draft, Writing - review & editing. **Marilyn Horta:** Methodology, Software, Investigation, Data curation, Writing - review & editing. **Ian Frazier:** Methodology, Software, Investigation, Data curation, Writing - review & editing. **Eliany Perez:** Investigation, Data curation, Writing - review & editing. **Marite Ojeda:** Investigation, Data curation, Writing - review & editing. **Eric Porges:** Methodology, Writing - review & editing. **Yenisel Cruz-Almeida:** Writing - review & editing. **David Feifel:** Writing - review & editing, Methodology, Resources. **Natalie C. Ebner:** Conceptualization, Software, Methodology, Investigation, Resources, Data curation, Writing - original draft, Writing - review & editing, Supervision, Project administration, Funding acquisition.

Declaration of Competing Interest

The authors declare that they have no known competing financial interests or personal relationships that could have appeared to influence the work reported in this paper.

Acknowledgments

The authors wish to thank the Social-Cognitive and Affective Developmental Lab and the faculty and staff at the Institute on Aging at the University of Florida for support in study logistics and data collection. The authors also thank the study pharmacist Dr. Susan E. Beltz and the study MD Dr. Bhanuprasad Sandesara for their roles in drug-related study logistics; and Dr. Jamie Morris for making the Heider-Simmel Task stimuli available. The authors are grateful to all participants for their contribution to this research.

Funding

This work was supported by the University of Florida Claude D. Pepper Older Americans Independence Center (grant P30AG028740), the College of Liberal Arts and Sciences, the Department of Psychology, and the Center for Cognitive Aging and Memory at University of Florida; the Pain Research and Intervention Center of Excellence-Clinical and Translational Science Institute-Institute on Aging grant ARG DTD 03-26-2008; the National Institute on Aging grant R01AG059809; the McKnight Brain Institute at the National High Magnetic Field Laboratory's AMRIS Facility, National Science Foundation, Division of Materials Research (grant number: 1157490), and the State of Florida; the National Institute on Aging Pre-Doctoral Fellowship on Physical, Cognitive, and Mental Health in Social Context (grant number: T32AG020499); the National Institute on Aging Post-Doctoral Fellowship on Integrative and Multidisciplinary Pain and Aging Research Training (grant number: 3T32AG049673-04); the UF Substance Abuse Training Center in Public Health from the National Institute of Drug Abuse (NIDA) of the National Institutes of Health (grant number: T32DA035167). Spray pumps were provided by Aptar Pharma and spray bottles by SGD Pharma.

Appendix A. Supplementary data

Supplementary data to this article can be found online at <https://doi.org/10.1016/j.nbas.2021.100023>.

References

- [1] J. Abdai, B. Ferdinandy, C.B. Terencio, Á. Pogány, Á. Miklósi, Perception of animacy in dogs and humans, *Biol Lett* 13 (6) (2017) 20170156, <https://doi.org/10.1098/rsbl.2017.0156>.
- [2] K. Alaerts, S. Bernaerts, J. Prinsen, C. Dillen, J. Steyaert, N. Wenderoth, Oxytocin induces long-lasting adaptations within amygdala circuitry in autism: a treatment-mechanism study with randomized placebo-controlled design, *Neuropsychopharmacology* 45 (7) (2020) 1141–1149, <https://doi.org/10.1038/s41386-020-0653-8>.
- [3] J. Ashburner, A fast diffeomorphic image registration algorithm, *Neuroimage* 38 (1) (2007) 95–113, <https://doi.org/10.1016/j.neuroimage.2007.07.007>.
- [4] J. Ashburner, K.J. Friston, Unified segmentation, *Neuroimage* 26 (3) (2005) 839–851, <https://doi.org/10.1016/j.neuroimage.2005.02.018>.
- [5] T. Atsumi, Y. Nagasaka, Y. Osada, The perception of animacy in humans and squirrel monkeys (*Saimiri sciureus*), *J Vis* 11 (11) (2011) 680, <https://doi.org/10.1167/11.11.680>.
- [6] Z. Bar-Joseph, D.K. Gifford, T.S. Jaakkola, Fast optimal leaf ordering for hierarchical clustering, *Bioinformatics* 17 (Suppl 1) (2001) S22–S29, https://doi.org/10.1093/bioinformatics/17.suppl_1.S22.

- [7] J.A. Barraza, N.S. Grewal, S. Ropacki, P. Perez, A. Gonzalez, P.J. Zak, Effects of a 10-day oxytocin trial in older adults on health and well-being, *Exp Clin Psychopharmacol* 21 (2013) 85–92, <https://doi.org/10.1037/a0031581>.
- [8] J.A. Bartz, J. Zaki, N. Bolger, K.N. Ochsner, Social effects of oxytocin in humans: context and person matter, *Trends Cogn Sci* 15 (2011) 301–309, <https://doi.org/10.1016/j.tics.2011.05.002>.
- [9] S. Bornaert, B. Boets, J. Steyaert, N. Wenderoth, K. Alaerts, Oxytocin treatment attenuates amygdala activity in autism: a treatment-mechanism study with long-term follow-up, *Transl Psychiatry* 10 (1) (2020), <https://doi.org/10.1038/s41398-020-01069-w>.
- [10] R.A.I. Bethlehem, J. van Honk, B. Auyeung, S. Baron-Cohen, Oxytocin, brain physiology, and functional connectivity: A review of intranasal oxytocin fMRI studies, *Psychoneuroendocrinology* 38 (7) (2013) 962–974, <https://doi.org/10.1016/j.psyneuen.2012.10.011>.
- [11] F. Binkofski, L.J. Buxbaum, Two action systems in the human brain, *Brain Lang* 127 (2) (2013) 222–229, <https://doi.org/10.1016/j.bandl.2012.07.007>.
- [12] S.J. Blakemore, P. Boyer, M. Pachot-Clouard, A. Meltzoff, C. Segebarth, J. Decety, The detection of contingency and animacy from simple animations in the human brain, *Cereb Cortex* 13 (2003) 837–844, <https://doi.org/10.1093/cercor/13.8.837>.
- [13] J. Born, T. Lange, W. Kern, G.P. McGregor, U. Bickel, H.L. Fehm, Sniffing neuropeptides: a transnasal approach to the human brain, *Nat Neurosci* 5 (6) (2002) 514–516, <https://doi.org/10.1038/nn0602-849>.
- [14] S. Bracci, J.B. Ritchie, I. Kalfas, H.P. Op de Beeck, The Ventral Visual Pathway Represents Animal Appearance over Animacy, Unlike Human Behavior and Deep Neural Networks, *J Neurosci* 39 (33) (2019) 6513–6525, <https://doi.org/10.1523/JNEUROSCI.1714-18.2019>.
- [15] J. Brandt, M. Spencer, M. Folstein, The telephone interview for cognitive status, *Neuropsychiatry, Neuropsychol Behav Neurol* 1 (1988) 111–117, <https://doi.org/10.1097/WNN.0000000000000166>.
- [16] K.S. Button, J.P.A. Ioannidis, C. Mokrysz, B.A. Nosek, J. Flint, E.S.J. Robinson, et al., Power failure: Why small sample size undermines the reliability of neuroscience, *Nat Rev Neurosci* 14 (5) (2013) 365–376, <https://doi.org/10.1038/nrn3475>.
- [17] A. Campbell, T. Ruffman, J.E. Murray, P. Glue, Oxytocin improves emotion recognition for older males, *Neurobiol Aging* 35 (10) (2014) 2246–2248, <https://doi.org/10.1016/j.neurobiolaging.2014.04.021>.
- [18] F. Castelli, F. Happé, U. Frith, C. Frith, Movement of mind: a functional imaging study of perception of perception and interpretation of complex intentional movement patterns Movement and Mind: A Functional Imaging Study of Perception and Interpretation of Complex Intentional Movement Patterns, *Neuroimage* 12 (2000) 314–325, <https://doi.org/10.1006/nimg.2000.0612>.
- [19] X.u. Chen, P.D. Hackett, A.C. DeMarco, C. Feng, S. Stair, E. Haroon, et al., Effects of oxytocin and vasopressin on the neural response to unreciprocated cooperation within brain regions involved in stress and anxiety in men and women, *Brain Imaging Behav* 10 (2) (2016) 581–593, <https://doi.org/10.1007/s11682-015-9411-7>.
- [20] C. Cheng, L. Fan, X. Xia, S.B. Eickhoff, H. Li, H. Li, et al., Rostro-caudal organization of the human posterior superior temporal sulcus revealed by connectivity profiles, *Hum Brain Mapp* 39 (12) (2018) 5112–5125, <https://doi.org/10.1002/hbm.v39.12.1002/hbm.24349>.
- [21] J. Chumbley, K. Worsley, G. Flandin, K. Friston, Topological FDR for neuroimaging, *Neuroimage* 49 (4) (2010) 3057–3064, <https://doi.org/10.1016/j.neuroimage.2009.10.090>.
- [22] R. Ciric, D.H. Wolf, J.D. Power, D.R. Roalf, G.L. Baum, K. Ruparel, et al., Benchmarking of participant-level confound regression strategies for the control of motion artifact in studies of functional connectivity, *Neuroimage* 154 (2017) 174–187, <https://doi.org/10.1016/j.neuroimage.2017.03.020>.
- [23] S. Dasgupta, R. Srinivasan, E.D. Grossman, Multivariate pattern analysis of the human pSTS: A comparison of three prototypical localizers, *Neuropsychologia* 120 (2018) 50–58, <https://doi.org/10.1016/j.neuropsychologia.2018.10.004>.
- [24] S. Dasgupta, S.C. Tyler, J. Wicks, R. Srinivasan, E.D. Grossman, Network Connectivity of the Right STS in Three Social Perception Localizers, *J Cogn Neurosci* 29 (2017) 221–234, https://doi.org/10.1162/jocn_a.01054.
- [25] N.C. Ebner, H. Chen, E. Porges, T. Lin, H. Fischer, D. Feifel, et al., Oxytocin's effect on resting-state functional connectivity varies by age and sex, *Psychoneuroendocrinology* 69 (2016) 50–59, <https://doi.org/10.1016/j.psyneuen.2016.03.013>.
- [26] N.C. Ebner, H. Fischer, Emotion and aging: Evidence from brain and behavior, *Front Psychol* 5 (2014), <https://doi.org/10.3389/fpsyg.2014.00996>.
- [27] N.C. Ebner, M. Horta, T. Lin, D. Feifel, H. Fischer, R.A. Cohen, Oxytocin modulates meta-mood as a function of age and sex, *Front Aging Neurosci* 7 (2015), <https://doi.org/10.3389/fnagi.2015.00175>.
- [28] N.C. Ebner, G.M. Maura, K. MacDonald, L. Westberg, H. Fischer, Oxytocin and socioemotional aging: Current knowledge and future trends, *Front Hum Neurosci* 7 (2013) 1–14, <https://doi.org/10.3389/fnhum.2013.00487>.
- [29] L. Fan, H. Li, J. Zhuo, Y.u. Zhang, J. Wang, L. Chen, et al., The Human Brainnetome Atlas: A New Brain Atlas Based on Connectome Architecture, *10.1093/cercor/bhw157*.
- [30] C. Feng, A. Lori, I.D. Waldman, E.B. Binder, E. Haroon, J.K. Rilling, A common oxytocin receptor gene (OXTR) polymorphism modulates intranasal oxytocin effects on the neural response to social cooperation in humans, *Genes, Brain Behav.* 14 (7) (2015) 516–525, <https://doi.org/10.1111/gbb.12234>.
- [31] K. Friston, *Experimental Design and Statistical Parametric Mapping, Human Brain Function: Second Edition.* (2003) 599–632, <https://doi.org/10.1016/B978-012264841-0/50033-0>.
- [32] I. Gordon, A. Jack, C.M. Pretzsch, B. Vander Wyk, J.F. Leckman, R. Feldman, et al., Intranasal Oxytocin Enhances Connectivity in the Neural Circuitry Supporting Social Motivation and Social Perception in Children with Autism, *Sci Rep* 6 (1) (2016), <https://doi.org/10.1038/srep35054>.
- [33] S.A. Grace, S.L. Rossell, M. Heinrichs, C. Kordsachia, I. Labuschagne, Oxytocin and brain activity in humans: A systematic review and coordinate-based meta-analysis of functional MRI studies, *Psychoneuroendocrinology* 96 (2018) 6–24, <https://doi.org/10.1016/j.psyneuen.2018.05.031>.
- [34] S.A. Grainger, J.D. Henry, H.R. Steinvik, E.J. Vanman, Intranasal oxytocin does not alter initial perceptions of facial trustworthiness in younger or older adults, *J Psychopharmacol* 33 (2) (2019) 250–254, <https://doi.org/10.1177/0269881118806303>.
- [35] S.A. Grainger, J.D. Henry, H.R. Steinvik, E.J. Vanman, P.G. Rendell, I. Labuschagne, Intranasal oxytocin does not reduce age-related difficulties in social cognition, *Horm Behav* 99 (2018) 25–34, <https://doi.org/10.1016/j.yhbeh.2018.01.009>.
- [36] A.J. Guastella, I.B. Hickie, M.M. McGuinness, M. Otis, E.A. Woods, H. M. Disinger, et al., Recommendations for the standardisation of oxytocin nasal administration and guidelines for its reporting in human research, *Psychoneuroendocrinology* 38 (5) (2013) 612–625, <https://doi.org/10.1016/j.psyneuen.2012.11.019>.
- [37] A.J. Guastella, C. MacLeod, A critical review of the influence of oxytocin nasal spray on social cognition in humans: Evidence and future directions, *Horm Behav* 61 (3) (2012) 410–418, <https://doi.org/10.1016/j.yhbeh.2012.01.002>.
- [38] X. Guell, J.D.E. Gabrieli, J.D. Schmahmann, Triple representation of language, working memory, social and emotion processing in the cerebellum: convergent evidence from task and seed-based resting-state fMRI analyses in a single large cohort, *Neuroimage* 172 (2018) 437–449, <https://doi.org/10.1016/j.neuroimage.2018.01.082>.
- [39] B. Guerra-Carrillo, A.P. Mackey, S.A. Bunge, Resting-state fMRI: A window into human brain plasticity, *Neuroscientist* 20 (5) (2014) 522–533, <https://doi.org/10.1177/1073858414524442>.
- [40] E.E. Hecht, D.L. Robins, P. Gautam, T.Z. King, Intranasal oxytocin reduces social perception in women: Neural activation and individual variation, *Neuroimage* 147 (2017) 314–329, <https://doi.org/10.1016/j.neuroimage.2016.12.046>.
- [41] F. Heider, Social perception and phenomenal causality, *Psychol Rev* 51 (6) (1944) 358–374, <https://doi.org/10.1037/h0055425>.
- [42] F. Heider, M. Simmel, An experimental study of social behavior, *Am J Psychol* 57 (1944) 243–259.
- [43] J.D. Henry, L.H. Phillips, T. Ruffman, P.E. Bailey, A meta-analytic review of age differences in theory of mind, *Psychol Aging* 28 (2013) 826–839, <https://doi.org/10.1037/a0030677>.
- [44] H. Hillebrandt, K.J. Friston, S.-J. Blakemore, Effective connectivity during animacy perception – dynamic causal modelling of Human Connectome Project data, *Sci Rep* 4 (2015) 6240, <https://doi.org/10.1038/srep06240>.
- [45] M. Horta, K. Kaylor, D. Feifel, N.C. Ebner, Chronic oxytocin administration as a tool for investigation and treatment: A cross-disciplinary systematic review, *Neurosci Biobehav Rev* 108 (2020) 1–23, <https://doi.org/10.1016/j.neubiorev.2019.10.012>.
- [46] Horta, M., Pehlivanoglu, D., Ebner, N.C., 2020b. The Role of Intranasal Oxytocin on Social Cognition: an Integrative Human Lifespan Approach. *Curr Behav Neurosci Reports* Doi: 10.1007/s40473-020-00214-5.
- [47] M. Horta, M. Ziaei, T. Lin, E.C. Porges, H. Fischer, D. Feifel, et al., Oxytocin alters patterns of brain activity and amygdalar connectivity by age during dynamic facial emotion identification, *Neurobiol Aging* 78 (2019) 42–51, <https://doi.org/10.1016/j.neurobiolaging.2019.01.016>.

- [48] L. Isik, K. Koldewyn, D. Beeler, N. Kanwisher, Perceiving social interactions in the posterior superior temporal sulcus, *Proc Natl Acad Sci* 114 (43) (2017) E9145–E9152, <https://doi.org/10.1073/pnas.1714471114>.
- [49] A. Jack, J.J. Connelly, J.P. Morris, DNA methylation of the oxytocin receptor gene predicts neural response to ambiguous social stimuli, *Front Hum Neurosci* 6 (2012) 1–7, <https://doi.org/10.3389/fnhum.2012.00280>.
- [50] M.H. Johnson, Biological Motion: A Perceptual Life Detector?, *Curr Biol* 16 (10) (2006) R376–R377, <https://doi.org/10.1016/j.cub.2006.04.008>.
- [51] M. Kanat, M. Heinrichs, G. Domes, Oxytocin and the social brain: Neural mechanisms and perspectives in human research, *Brain Res* 1580 (2014) 160–171, <https://doi.org/10.1016/j.brainres.2013.11.003>.
- [52] N. Khalili-Mahani, S.A.R.B. Rombouts, M.J.P. van Osch, E.P. Duff, F. Carbonell, L.D. Nickerson, et al., Biomarkers, designs, and interpretations of resting-state fMRI in translational pharmacological research: A review of state-of-the-Art, challenges, and opportunities for studying brain chemistry, *Hum Brain Mapp* 38 (4) (2017) 2276–2325, <https://doi.org/10.1002/hbm.23516>.
- [53] J.M. Kilner, More than one pathway to action understanding, *Trends Cogn Sci* 15 (8) (2011) 352–357, <https://doi.org/10.1016/j.tics.2011.06.005>.
- [54] T. Konkle, A. Caramazza, Tripartite organization of the ventral stream by animacy and object size, *J Neurosci* 33 (25) (2013) 10235–10242, <https://doi.org/10.1523/JNEUROSCI.0983-13.2013>.
- [55] J. Kou, Y. Zhang, F. Zhou, C. Sindermann, C. Montag, B. Becker, et al., A randomized trial shows dose-frequency and genotype may determine the therapeutic efficacy of intranasal oxytocin, *Psychol Med* (2020), <https://doi.org/10.1017/S0033291720003803>.
- [56] B. Kovács, S. Kéri, Off-label intranasal oxytocin use in adults is associated with increased amygdala-cingulate resting-state connectivity, *Eur Psychiatry* 30 (2015) 542–547, <https://doi.org/10.1016/j.eurpsy.2015.02.010>.
- [57] A.R. Laird, P.M. Fox, S.B. Eickhoff, J.A. Turner, K.L. Ray, D.R. McKay, et al., Behavioral interpretations of intrinsic connectivity networks, *J Cogn Neurosci* 23 (2011) 4022–4037, https://doi.org/10.1162/jocn_a_00077.
- [58] K. Lancaster, C.S. Carter, H. Pournajafi-Nazarloo, T. Karaoli, T.S. Lillard, A. Jack, et al., Plasma oxytocin explains individual differences in neural substrates of social perception, *Front Hum Neurosci* 9 (2015) 132, <https://doi.org/10.3389/fnhum.2015.00132>.
- [59] M.R. Lee, K.B. Scheidweiler, X.X. Diao, F. Akhlaghi, A. Cummins, M.A. Huestis, et al., Oxytocin by intranasal and intravenous routes reaches the cerebrospinal fluid in rhesus macaques: Determination using a novel oxytocin assay, *Mol Psychiatry* 23 (2018) 115–122, <https://doi.org/10.1038/mp.2017.27>.
- [60] A. Lingnau, P.E. Downing, The lateral occipitotemporal cortex in action, *Trends Cogn Sci* (2015), <https://doi.org/10.1016/j.tics.2015.03.006>.
- [61] K. MacDonald, D. Feifel, Helping oxytocin deliver: Considerations in the development of oxytocin-based therapeutics for brain disorders, *Front Neurosci* (2013), <https://doi.org/10.3389/fnins.2013.00035>.
- [62] D.A. Martins, N. Mazibuko, F. Zelaya, S. Vasilakopoulou, J. Loveridge, A. Oates, et al., Effects of route of administration on oxytocin-induced changes in regional cerebral blood flow in humans, *Nat Commun* 11 (2020), <https://doi.org/10.1038/s41467-020-14845-5>.
- [63] D.G. McLaren, M.L. Ries, G. Xu, S.C. Johnson, A generalized form of context-dependent psychophysiological interactions (gPPI): A comparison to standard approaches, *Neuroimage* 61 (2012) 1277–1286, <https://doi.org/10.1016/j.neuroimage.2012.03.068>.
- [64] A.D. Milner, M.A. Goodale, Two visual systems re-viewed, *Neuropsychologia* 46 (2008) 774–785, <https://doi.org/10.1016/j.neuropsychologia.2007.10.005>.
- [65] J.M. Moran, E. Jolly, J.P. Mitchell, Social-cognitive deficits in normal aging, *J Neurosci* 32 (2012) 5553–5561, <https://doi.org/10.1523/jneurosci.5511-11.2012>.
- [66] M. Pagani, A. De Felice, C. Montani, A. Galbusera, F. Papaleo, A. Gozzi, Acute and Repeated Intranasal Oxytocin Differentially Modulate Brain-wide Functional Connectivity, *Neuroscience* (2020), <https://doi.org/10.1016/j.neuroscience.2019.12.036>.
- [67] D.S. Quintana, A. Lischke, S. Grace, D. Scheele, Y. Ma, B. Becker, Advances in the field of intranasal oxytocin research: lessons learned and future directions for clinical research, *Mol Psychiatry* (2020), <https://doi.org/10.1038/s41380-020-00864-7>.
- [68] D.S. Quintana, J. Rokicki, D. van der Meer, D. Alnæs, T. Kaufmann, A. Córdova-Palomeria, et al., Oxytocin pathway gene networks in the human brain, *Nat Commun* 10 (2019), <https://doi.org/10.1038/s41467-019-08503-8>.
- [69] D.S. Quintana, L.T. Westlye, D. Alnæs, Ø.G. Rustan, T. Kaufmann, K.T. Smerud, et al., Low dose intranasal oxytocin delivered with Breath Powered device dampens amygdala response to emotional stimuli: A peripheral effect-controlled within-subjects randomized dose-response fMRI trial, *Psychoneuroendocrinology* 69 (2016) 180–188, <https://doi.org/10.1016/j.psyneuen.2016.04.010>.
- [70] J.K. Rilling, A.C. DeMarco, P.D. Hackett, X. Chen, P. Gautam, S. Stair, et al., Sex differences in the neural and behavioral response to intranasal oxytocin and vasopressin during human social interaction, *Psychoneuroendocrinology* 39 (2014) 237–248, <https://doi.org/10.1016/j.psyneuen.2013.09.022>.
- [71] B.Z. Roberts, J.W. Young, Y.V. He, Z.A. Cope, P.D. Shilling, D. Feifel, Oxytocin improves probabilistic reversal learning but not effortful motivation in Brown Norway rats, *Neuropharmacology* 150 (2019) 15–26, <https://doi.org/10.1016/j.neuropharm.2019.02.028>.
- [72] P. Rochat, R. Morgan, M. Carpenter, Young infants' sensitivity to movement information specifying social causality, *Cogn. Dev.* 12 (1997) 537–561, [https://doi.org/10.1016/S0885-2014\(97\)90022-8](https://doi.org/10.1016/S0885-2014(97)90022-8).
- [73] T. Ruffman, J.D. Henry, V. Livingstone, L.H. Phillips, A meta-analytic review of emotion recognition and aging: Implications for neuropsychological models of aging, *Neurosci Biobehav Rev* 32 (2008) 863–881, <https://doi.org/10.1016/j.neubiorev.2008.01.001>.
- [74] J.M. Rung, M. Horta, E.M. Tammi, E. Perez, M.C. Ojeda, T. Lin, et al., Safety and tolerability of chronic intranasal oxytocin in older men: results from a randomized controlled trial, *Psychopharmacology* (2021), <https://doi.org/10.1007/s00213-021-05862-3>.
- [75] Sannino, S., Chini, B., Grinevich, V., 2017. Lifespan oxytocin signaling: Maturation, flexibility, and stability in newborn, adolescent, and aged brain. *Dev. Neurobiol.* Doi: 10.1002/dneu.22450.
- [76] D. Scheele, C. Schwering, J.T. Ellison, R. Spunt, W. Maier, R. Hurlmann, A human tendency to anthropomorphize is enhanced by oxytocin, *Eur Neuropsychopharmacol* 25 (2015) 1817–1823, <https://doi.org/10.1016/j.euroneuro.2015.05.009>.
- [77] R.T. Schultz, D.J. Grelotti, A. Klin, J. Kleinman, C. Van Der Gaag, R. Marois, et al., The role of the fusiform face area in social cognition: Implications for the pathobiology of autism, *Philos Trans R Soc B Biol Sci* 358 (2003) 415–427, <https://doi.org/10.1098/rstb.2002.1208>.
- [78] S.H. Seeley, Y. Chou, M.-F. O'Connor, Intranasal Oxytocin and OXTR Genotype Effects on Resting State Functional Connectivity: A Systematic Review, *Neurosci Biobehav Rev* 95 (2018) 17–32, <https://doi.org/10.1016/j.neubiorev.2018.09.011>.
- [79] S.G. Shamy-Tsoory, A. Abu-Akel, The Social Salience Hypothesis of Oxytocin, *Biol Psychiatry* 79 (2016) 194–202, <https://doi.org/10.1016/j.biopsych.2015.07.020>.
- [80] S.M. Smith, T.E. Nichols, Threshold-free cluster enhancement: Addressing problems of smoothing, threshold dependence and localisation in cluster inference, *Neuroimage* 44 (2009) 83–98, <https://doi.org/10.1016/j.neuroimage.2008.03.061>.
- [81] R.P. Spunt, M.D. Lieberman, The Busy Social Brain: Evidence for Automaticity and Control in the Neural Systems Supporting Social Cognition and Action Understanding, *Psychol Sci* 24 (2013) 80–86, <https://doi.org/10.1177/0956797612450884>.
- [82] M. Sugiura, Functional neuroimaging of normal aging: Declining brain, adapting brain, *Ageing Res. Rev.* (2016), <https://doi.org/10.1016/j.arr.2016.02.006>.
- [83] P. Tavares, A.D. Lawrence, P.J. Barnard, Paying Attention to Social Meaning: An fMRI Study, *Cereb Cortex* 18 (2008) 1876–1885, <https://doi.org/10.1093/cercor/bhm212>.
- [84] N. Tzourio-con, B. Landeau, D. Papathanassiou, F. Crivello, O. Etard, N. Delcroix, et al., Automated Anatomical Labeling of Activations in SPM Using a Macroscopic Anatomical Parcellation of the MNI MRI Single-Subject Brain, *Neuroimage* 15 (2002) 273–289, <https://doi.org/10.1006/nimg.2001.0978>.
- [85] J. Walbrin, P. Downing, K. Koldewyn, Neural responses to visually observed social interactions, *Neuropsychologia* 112 (2018) 31–39, <https://doi.org/10.1016/j.neuropsychologia.2018.02.023>.
- [86] T. Watanabe, M. Kuroda, H. Kuwabara, Y. Aoki, N. Iwashiro, N. Tatsunobu, et al., Clinical and neural effects of six-week administration of oxytocin on core symptoms of autism, *Brain* 138 (2015) 3400–3412, <https://doi.org/10.1093/brain/awv249>.
- [87] S. Whitfield-Gabrieli, A. Nieto-Castanon, Conn: A Functional Connectivity Toolbox for Correlated and Anticorrelated Brain Networks, *Brain Connect* 2 (2012) 125–141, <https://doi.org/10.1089/brain.2012.0073>.
- [88] D.Y.J. Yang, G. Rosenblau, C. Keifer, K.A. Pelphrey, An integrative neural model of social perception, action observation, and theory of mind, *Neurosci Biobehav Rev* (2015), <https://doi.org/10.1016/j.neubiorev.2015.01.020>.